Hindawi
International Journal of Antennas and Propagation
Volume 2024, Article ID 9055869, 13 pages
https://doi.org/10.1155/2024/9055869

Research Article

Phase Error Criterion Based Adaptive Algorithm for Frequency Estimation

Prayuth Inban,[1] **Rachu Punchalard**,[2] **and Chawalit Benjangkaprasert**[3]

[1]*School of Engineering, King Mongkut's Institute of Technology Ladkrabang, Bangkok, Thailand*
[2]*School of Electrical Engineering, Faculty of Industrial Technology, Rajabhat Rajanagarindra University, Chachoengsao, Thailand*
[3]*Department of Computer Engineering, School of Engineering, King Mongkut's Institute of Technology Ladkrabang, Bangkok, Thailand*

Correspondence should be addressed to Prayuth Inban; prayuth@techno.rru.ac.th

Received 10 March 2023; Revised 17 February 2024; Accepted 8 March 2024; Published 18 March 2024

Academic Editor: Khaled Rouabah

A simple phase error criterion (PEC-)-based adaptive algorithm for estimating the frequency of a complex sinusoidal signal in additive white Gaussian and impulsive noises is proposed. The proposed technique makes use of the instantaneous phase response of a first-order complex linear predictor (CLP) as a driving function to update the frequency parameter of the CLP. The proposed PEC is attractive due to its simplicity and high impulsive noise robustness. Theoretical analysis for the mean value of the estimated frequency and the steady-state mean square error (MSE) of the frequency estimate are derived in closed forms. Computer simulations are drawn to show the performance of the proposed frequency estimator.

1. Introduction

Adaptive method-based frequency estimation can be found in many areas of digital signal processing applications [1, 2], such as Doppler effect estimation of radar and sonar systems [3–5], clock and carrier synchronization in communication systems, angle of arrival estimation in smart antenna systems, frequency estimation in global navigation satellite systems (GNSS) [6], angle and frequency estimation in cognitive wireless systems [7–9], and so on. Depending on the statistical properties of the input signal frequency, say, deterministic or random, the frequency estimation can be classified into two categories: block-based and sequential-based estimation techniques. The multiple signal classification (MUSIC) [9], the modified covariance (MC) [10], the Pisarenko harmonic decomposition (PHD) [11], the reformed PHD [12], and the maximum likelihood estimation (ML) [13] are examples of block estimation that are used for estimating an unknown constant sinusoidal signal frequency. However, since the required computational cost of those techniques is high, many methods have been adopted to overcome this drawback [14, 15]. For the time-varying sinusoidal signal frequency estimation, sequential-based estimation techniques such as the three recursive least-squares (RLS) algorithms [16] and the least-mean-square (LMS) family algorithm [17] is required. In [17], So and Ching proposed the real direct frequency estimation (RDFE) adaptive algorithm for a real tone in noise. The RDFE is based on the linear prediction of real sinusoidal signals [18]. The RDFE is computationally efficient, and it provides unbiased and direct frequency measurements on a sequential basis. In the case of a complex sinusoidal signal frequency estimation, the block-based estimations [19–22] and the complex adaptive notch filter (CANF)-based adaptive algorithms [23–26] can be applied. In [23], the modified complex plain gradient (MCPG) adaptive algorithm was adopted. It was found that the MCPG can improve convergence speed as compared with those of the Regalia method (Regalia) [24] and the complex plain gradient (CPG) algorithm [26] without increasing any computations. However, due to the pole contraction factor of the CANF, the performance of an adaptive algorithm-based adaptive

ANF may be poor if the selected value of the pole factor is inappropriate. In [27], the linear prediction-based adaptive algorithm [17] is adopted for the general case of a complex sinusoidal signal, namely, a complex direct frequency estimation (CDFE). The CDFE is an interesting algorithm because of its simplicity and efficiency. However, it provides slow convergence speeds when the signal amplitude is low and is not robust to high impulsive noise.

In this work, we propose a very simple sequential phase error criterion (PEC-)-based adaptive algorithm to estimate the frequency of a complex sinusoid. An instantaneous phase of a complex linear predictor is evaluated at each time instant and used to be the driving function of the algorithm. The proposed PEC does not require any external or internal signals; only the input and output signals of the system are required. In some conditions, the PEC gives a similar convergence time and MSE to those of the CDFE but is more robust to impulsive noise. In close form, convergence analysis for convergence in the mean of the estimated frequency and steady-state MSE under white Gaussian noise is derived. Extensive simulations under Gaussian and impulsive noise scenarios are evaluated to demonstrate the superiority of the proposed PEC.

2. Algorithm Derivation

It is assumed that the observation signal of the proposed algorithm takes the form of the following equation:

$$x(n) = d(n) + v(n), \tag{1}$$

where $d(n) = Ae^{j(\omega_0 n+\varphi)}$, $A > 0$, $\omega_0 \in (-\pi, \pi)$, and $\varphi \in [-\pi, \pi]$ are, respectively, unknown amplitude, frequency, and phase. A and ω_0 can be constant or time varying whereas φ is uniformly distributed. $v(n) = v_r(n) + jv_i(n)$ is a zero-mean complex white Gaussian noise with variance σ^2 where $v_r(n)$ and $v_i(n)$ are uncorrelated real white processes with zero mean and identical variance of $\sigma^2/2$. The input signal to noise ratio (SNR_i) can be computed by $\mathrm{SNR}_i = A^2/\sigma^2$.

The objective of this work is to estimate ω_0 from the observation time series $x(n)$, according to the following adaptive rule:

$$\hat{\omega}_0(n+1) = \hat{\omega}_0(n) + \mu D(n), \tag{2}$$

where $\hat{\omega}_0(n)$ is the estimate at time n of ω_0, $\mu > 0$ is the step-size parameter controlling the speed of convergence; and $D(n)$ is an instantaneous driving function that must satisfy the following criteria:

$$D \equiv \begin{cases} E[D(n)] > 0, & \hat{\omega}_0(n) < \omega_0, \\ E[D(n)] < 0, & \hat{\omega}_0(n) > \omega_0, \\ E[D(n)] = 0, & \hat{\omega}_0(n) = \omega_0, \end{cases} \tag{3}$$

where $E[\cdot]$ is an expectation operator. To explore the aspect of D that satisfies equation (3), we consider the linear prediction of the signal [27]

$$s(n) = -e^{j\omega_0} s(n-1), \tag{4}$$

where the prediction error is defined by

$$e(n) = x(n) - \hat{s}(n), \tag{5}$$

and

$$\hat{s}(n) = -e^{j\hat{\omega}_0} x(n-1), \tag{6}$$

is the estimate of $s(n)$ and $\hat{\omega}_0$ is adjusted using equation (2). Note that the signal $s(n)$ in equation (4) and its estimated version $\hat{s}(n)$ in equation (6) are defined as a negative value to obtain a linear phase prediction error signal $e(n)$. Now let us define a new phase error criterion (PEC) as follows:

$$D \equiv E[D(n)] = \angle E\left[x(n)e^*(n)\right], \tag{7}$$

where

$$D(n) = \angle x(n)e^*(n), \tag{8}$$

the symbol $\angle$ is the phase operator, and the asterisk $(*)$ stands for the complex conjugation. In practice the instantaneous linear phase $D(n)$ can be calculated by

$$D(n) = \arctan \frac{\mathrm{Im}\left(x(n)e^*(n)\right)}{\mathrm{Re}\left(x(n)e^*(n)\right)}, \tag{9}$$

where $\mathrm{Im}(\cdot)$ is the imaginary part and $\mathrm{Re}(\cdot)$ is the real part. To study the behavior of $D(n)$, we put $x(n)$, $e(n)$, and $\hat{s}(n)$ into equation (7), yielding (see Appendix A)

$$\begin{aligned} D &= \angle\left(E\left[x(n)x^*(n) - x(n)\hat{s}^*(n)\right]\right) \\ &= -\arctan \frac{A^2 \sin\delta_\omega}{A^2\left(1 + \cos\delta_\omega\right) + \sigma^2}, \end{aligned} \tag{10}$$

where $\delta_\omega = \hat{\omega}_0 - \omega_0$ is an estimation error. It is obvious that $\hat{\omega}_0 = \omega_0$ is a stationary point of equation (10). To assert the validity of equation (10), the estimate of D based on Monte Carlo simulation is studied by using computer simulations. The parameters used in simulations include $\omega_0 = 0.5\pi$, $\varphi = 0.2\pi$, and the data length of $L = 10^4$. The driving function D as a function of frequency parameter $\hat{\omega}_0$ for different values of SNR_i are depicted in Figure 1. It is observed that the analytical and simulated results are well consistent for both low and high values of SNR_i and they satisfy the desired criteria in equation (3). As a result, the convergence of equation (2) is ensured if the proposed driving function in equation (8) is employed. Moreover, the closed form expression for D in equation (10) can be used to study the convergence behaviour of equation (2) because it is consistent with the simulations. Finally, by substituting equation (8) into (2) the proposed PEC adaptive algorithm is ultimately derived as follows:

$$\hat{\omega}_0(n+1) = \hat{\omega}_0(n) + \mu\angle x(n)e^*(n). \tag{11}$$

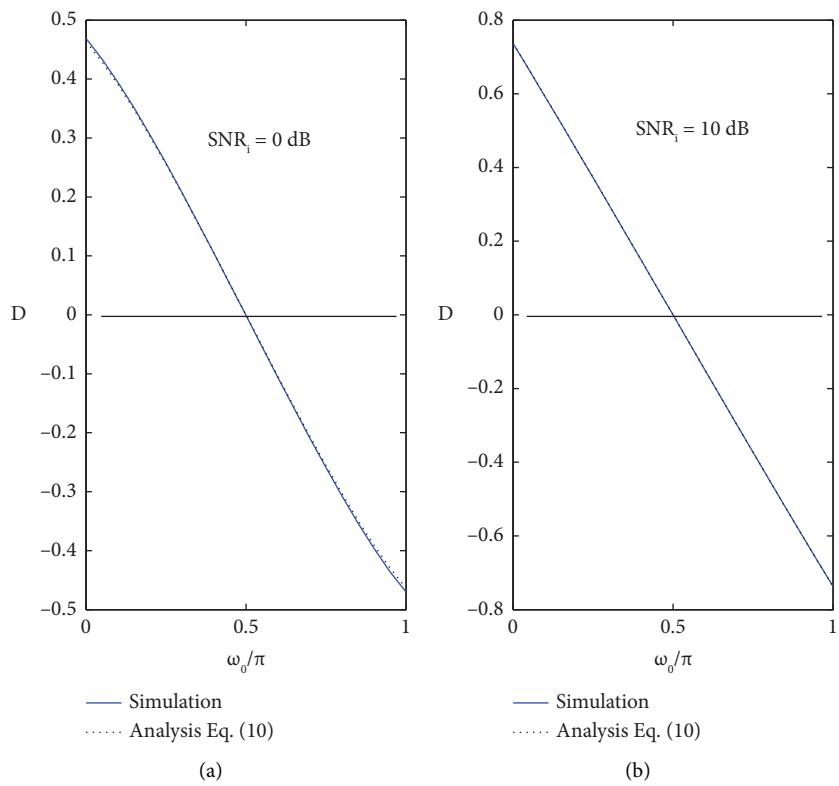

Figure 1: Expected value of the PEC driving function D as a function of frequency parameter for (a) $\mathrm{SNR}_i = 0$ dB; (b) $\mathrm{SNR}_i = 10$ dB.

As has been observed, the proposed PEC algorithm is very simple and attractive because no internal and external additional signals are required to update the frequency parameter $\hat{\omega}_0$ of the CLP; only $x(n)$, $e(n)$, and a phase evaluator $\angle$ are required. Figure 2 shows the block diagram of the proposed estimator. In the next section, the convergence properties of the proposed PEC is addressed.

3. Mean Analysis

At steady-state $\hat{\omega}_0 \approx \omega_0$ the terms $\sin a|_{a\longrightarrow 0} \approx a$ and $\cos a|_{a\longrightarrow 0} \approx 1$, equation (10) can be approximated to be

$$D \approx -\arctan \frac{A^2 \delta_\omega}{2A^2 + \sigma^2}. \tag{12}$$

At a stationary point, the term $\delta_\omega \approx 0$, therefore, $\arctan u|_{u\longrightarrow 0} \approx u$, equation (12) can be simplified to be

$$D \approx -\frac{A^2 \delta_\omega}{2A^2 + \sigma^2}. \tag{13}$$

In order to study the mean value of equation (11), the steady-state expression for D in equation (13) is substituted into equation (11). After taking the expectation operator and using $\delta_\omega = \hat{\omega}_0 - \omega_0$, then equation (11) becomes

$$\bar{\omega}_0(n+1) = (1 - \mu\eta_0)\bar{\omega}_0(n) + \mu\eta_0\omega_0, \tag{14}$$

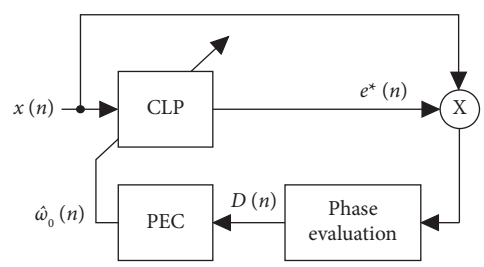

Figure 2: Block diagram of the proposed PEC.

where $\bar{\omega}_0(n) \equiv E[\hat{\omega}_0(n)]$ is an expected value of $\hat{\omega}_0(n)$ and

$$\eta_0 = \frac{A^2}{2A^2 + \sigma^2}. \tag{15}$$

Equation (14) is in the form of a first-order time-invariant difference equation in variable $\bar{\omega}_0(n)$ whose solution is given by (see Appendix B)

$$\bar{\omega}_0(n) = \left(\bar{\omega}_0(0) - \omega_0\right)(1 - \mu\eta_0)^n + \omega_0, \tag{16}$$

where $\bar{\omega}_0(0) \equiv \hat{\omega}_0(0)$ is an initial value of the frequency parameter $\hat{\omega}_0(n)$. Since $\mu\eta_0$ must be less than one, the term $(1 - \mu\eta_0) \longrightarrow 0$ as $n \longrightarrow \infty$, and equation (16) becomes

$$\bar{\omega}_0(n)|_{n\longrightarrow\infty} = \omega_0. \tag{17}$$

It is revealed from equation (17) that the proposed PEC algorithm converges to the desired solution and is unbiased. In addition, the convergence time of equation (11) can be predicted by using the fact that the term $(1-\mu\eta_0)$ will exponentially decrease in time, which can indicate that

$$(1-\mu\eta_0) = e^{-(1/\tau)}, \tag{18}$$

where τ is defined as a time constant. Solving equation (18) for τ yields

$$\tau = -\frac{1}{\log_e(1-\mu\eta_0)}. \tag{19}$$

According to equation (19), the approximate convergence time of the proposed PEC will be

$$L_i \approx 5\tau\,(\text{samples}). \tag{20}$$

Moreover, the stability bound of step-size in the mean sense can be easily obtained from equation (14) as follows:

$$0 < \mu < \frac{2}{\eta_0}. \tag{21}$$

The upper bound of step-size in equation (21) guarantees monotonic convergence in the mean sense. The validity of equations (16), (17), and (20) is tested by using the Monte Carlo simulation technique. A random experiment of 1000 trials for a random phase signal and a random noise sequence with a particular variance is carried out. The obtained 1000 frequency estimates are ensemble averaged to obtain the mean estimated frequency $\bar{\omega}_0(n)$. Figure 3 shows the learning curves of $\bar{\omega}_0(n)$ obtainable by equation (16) and simulations for $\text{SNR}_i = 0$ and 10 dB, $\omega_0 = 0.5\pi$, data length $L = 1000$, and $\mu = 0.05$. Note that all samples of the selected parameters used in simulating are defined based on the trial-and-error technique to obtain the best results. The step-size μ is confined within the range of equation (21). It is seen that the analytical result for $\bar{\omega}_0(n)$ shown in equation (16) can track those of the simulations very well in both low (0 dB) and high (10 dB) values of SNR_i and converge to solution as desired. By using equation (20), the convergence time is $L_i \approx 298$ samples at $\text{SNR}_i = 0$ dB and $L_i \approx 208$ samples at $\text{SNR}_i = 10$ dB which are close to those obtained from the simulations.

4. Steady-State MSE Analysis

In this section, MSE of the frequency estimate $\hat{\omega}_0(n)$ is analyzed. To do this task, the steady-state expression for the prediction error $e(n)$ is required. The input $x(n)$ to the prediction error $e(n)$ can be modelled by the following transfer function:

$$H(z) = 1 + e^{j\omega_0} z^{-1}. \tag{22}$$

Substituting $z = e^{j\omega}$, $\omega \in [-\pi, \pi]$ in equation (22) yields

$$H(\omega) = 1 + e^{-j(\omega-\omega_0)}. \tag{23}$$

If we replace $\omega \Rightarrow \hat{\omega}_0$, equation (23) becomes

$$\begin{aligned} H(\omega) &= 1 + e^{-j\delta_\omega} \\ &= 1 + \cos\delta_\omega - j\sin\delta_\omega. \end{aligned} \tag{24}$$

At steady-state $\hat{\omega}_0 \approx \omega_0$, the magnitude and phase responses of $H(z)$ can be, respectively, approximated to be

$$B_H = |H(\omega)| \approx 2, \tag{25}$$

and

$$\varphi_H \approx -\frac{\delta_\omega}{2}. \tag{26}$$

Therefore, the steady-state expression for the prediction error will be

$$e_s(n) = AB_H e^{j(\omega_0 n + \varphi + \varphi_H)} + v_1(n), \tag{27}$$

where s means steady-state and $v_1(n)$ is the noise component due to the input noise $v(n)$. Now let us consider the learning increment

$$Q = E\left[x(n)e_s^*(n)\right] = A^2 B_H e^{-j\varphi_H} + R_{vv_1^*}, \tag{28}$$

where

$$R_{vv_1^*} = E\left[v(n)v_1^*(n)\right] = \sigma^2, \tag{29}$$

is the correlation between $v(n)$ and $v_1^*(n)$ (see Appendix C). Note that the derivation of equation (28) is obtained by assuming that the input complex sinusoids and noise components are uncorrelated with each other [28]. Now, let us consider the SNR of Q, which is

$$\text{SNR}_Q = B_H \text{SNR}_i. \tag{30}$$

For a high value of SNR_Q equation (28) can be approximated as [29]

$$Q(n) \approx A^2 B_H e^{-j(\varphi_H + v_2(n))}, \tag{31}$$

where $Q(n)$ is the estimate of Q and $v_2(n)$ is defined as a phase noise of Q with zero mean and variance of [29]

$$\sigma_2^2 \approx \frac{1}{2\text{SNR}_Q} = \frac{1}{2B_H \text{SNR}_i}. \tag{32}$$

The phase of $Q(n)$ that is equivalent to the driving function D in equation (13) can be defined by

$$D_q(n) = \angle Q(n) = -\left(\varphi_H + v_2(n)\right). \tag{33}$$

Using equations (33) in (11) results in

$$\hat{\omega}_0(n+1) = \hat{\omega}_0(n) - \mu\left(\varphi_H + v_2(n)\right). \tag{34}$$

Subtracting ω_0 from both sides of equation (34) and using equation (26) yields

$$\delta_\omega(n+1) = \delta_\omega(n) - \mu\left(\frac{\delta_\omega(n)}{2} + v_2(n)\right). \tag{35}$$

Squaring on both sides of equation (35) and averaging the result gives

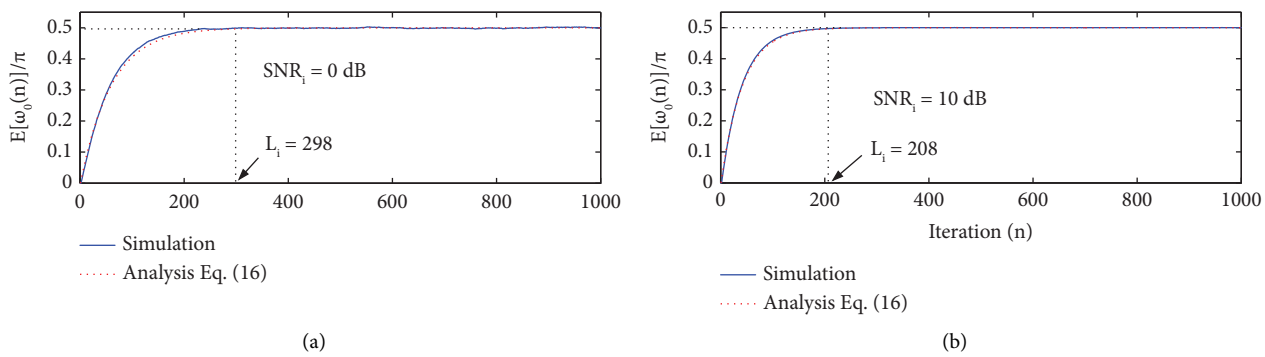

Figure 3: Leaning curves of $\overline{\omega}_0(0)$ for (a) $\mathrm{SNR}_i = 0$ dB; (b) $\mathrm{SNR}_i = 10$ dB.

$$\overline{\delta}_\omega^2(n+1) = \left(1 - \mu + \frac{\mu^2}{4}\right)\overline{\delta}_\omega^2(n) + \mu^2\sigma_2^2, \tag{36}$$

where $\overline{\delta}_\omega^2(n) = E[\delta_\omega^2(n)]$ is the estimation MSE at time n. Assuming that

$$\overline{\delta}_\omega^2(n+1)|_{n\longrightarrow\infty} = \overline{\delta}_\omega^2(n)|_{n\longrightarrow\infty} = \overline{\delta}_\omega^2(\infty), \tag{37}$$

then equation (36) becomes

$$\overline{\delta}_\omega^2(\infty) = \frac{\mu\sigma_2^2}{1-(\mu/4)} = \mathrm{MSE}. \tag{38}$$

For slow convergence speed when $\mu \longrightarrow 0$, equation (38) can be simplified to be

$$\mathrm{MSE} \approx \mu\sigma_2^2. \tag{39}$$

It is apparent that the MSE approximation in equation (39) is valid for a wide range of system parameters, including input frequency, SNR_i and step-size as demonstrated in Figures 4–6, respectively. It is observed that the analytical MSE shown in equation (39) can well predict the simulated MSE. It is observed that the MSE is independent of the signal frequency, as shown Figure 4, decreased as SNR_i increased, as shown in Figure 5, and increased as step-size increased, as shown in Figure 6.

5. Numerical Examples

In this section, the performances of the proposed PEC have been revealed and compared with those of the MCPG [23], Regalia [24], CPG [26], and CDFE [27].

5.1. Simulation MSE and Estimated Frequency. To fairly compare the MSE and the estimated frequency by using computer simulation, all examined algorithms are forced to converge at the same time. This is done by individually tuning the step-size parameter of each algorithm. In addition, the 1000 complex sinusoids with a specific frequency and random phase plus noise sequences having the same SNR_i are evaluated by using an ensemble average. The results are shown in Figures 7–10. Figure 7 is an estimation MSE comparison for $\mathrm{SNR}_i = 10$ dB (high SNR_i). It is revealed that the proposed PEC and CDFE converge at the same time, and they provide an identical MSE of the estimated frequency, whereas the MCPG converges the fastest and the Regalia shows the slowest. The CPG speed of convergence is slightly better than that of the Regalia but worse than those of the PEC, CDFE, and MCPG. Figure 8 demonstrates the estimation frequency at the same MSE. As can be seen, the PEC, CDFE, and MCPG provide almost the same convergence speed, whereas the CPG and Regalia show slow convergence speeds. Figure 9 is an estimation MSE comparison for $\mathrm{SNR}_i = -5$ dB (low SNR_i). It is shown that the convergence speed of the proposed PEC is between those of the CDFE and MCPG and the CPG and Regalia. Figure 10 shows the estimation frequency at the same MSE. As has been observed, the PEC provides slower speed than CDFE and MCPG but yields faster speed than the CPG and Regalia. Note that the MCPG, CPG, and Regalia are used with a complex first-order adaptive IIR notch filter (CANF) [26], which has a zero-pole contraction factor α. In this section, we let $\alpha = 0.9$. Although the convergence speed of the PEC in the additive complex white Gaussian noise scenario is slow as compared with the MCPG and CDFE, as shown in Figures 9 or 10, it performs well when exposed to a high-impulsive noise environment, as shown in Section 5.2. In addition, the deterioration of convergence speed due to the signal amplitude A does not affect the PEC, as shown in Section 5.3. Moreover, in the comparison of the calculation requirements of all algorithms, the computational complexity is concluded in Table 1. It is found that the proposed PEC requires only $3L$ multiplications, $2L$ additions, and L phase evaluations. The added phase calculation makes PEC tolerant to impulsive noise and insensitive to signal amplitude A, surpassing CDFE, MCPG, CPG, and Regalia. Now let us consider the computational time required for all examined algorithms. Since each algorithm has only one parameter (weight) to be adjusted, for the PEC, it requires six operations per iteration. This indicates that the PEC is considered to have a temporal complexity of order $O(6L)$ when its iteration has an input size of L. Because runtime is dependent on input size L, it is said that the time complexity of the PEC has an order of $O(L)$, meaning that it is linear. Similarly for the CDFE, MCPG, CPG, and Regalia, their computation times are also linear and are shown in Table 1. Although the runtime of each comparative algorithms has the same order as that of the PEC, the proposed PEC outperforms all

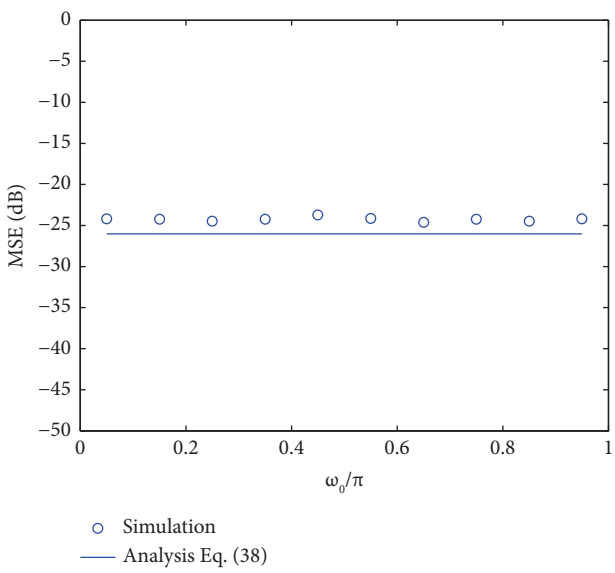

Figure 4: MSE as a function of frequency for $\mathrm{SNR}_i = 0\,\mathrm{dB}$, $\mu = 0.01$, $L = 10000$ and 100 runs.

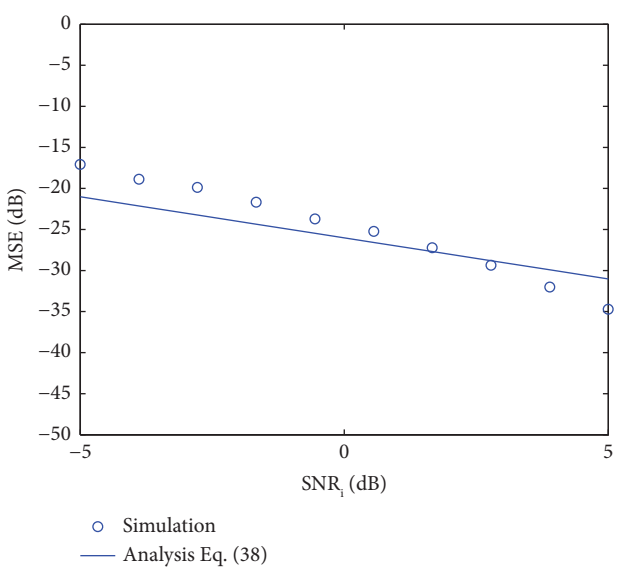

Figure 5: MSE as a function of SNR_i for $\omega_0 = 0.5\pi$, $\mu = 0.01$, $L = 10000$ and 100 runs.

comparative techniques in terms of impulsive noise robustness, and its convergence time is not sensitive to the input signal amplitude (see Figure 11).

5.2. Impulsive Noise Robustness. In this section, the impulsive noise robustness of the proposed PEC algorithm is addressed. It is well known that impulsive noise has two main characteristics: random amplitudes and places of occurrence. When impulsive noise is present, the noise power is equal to the strength of the impulse. This illustrates the nonstationary character of impulsive noise by looking at the

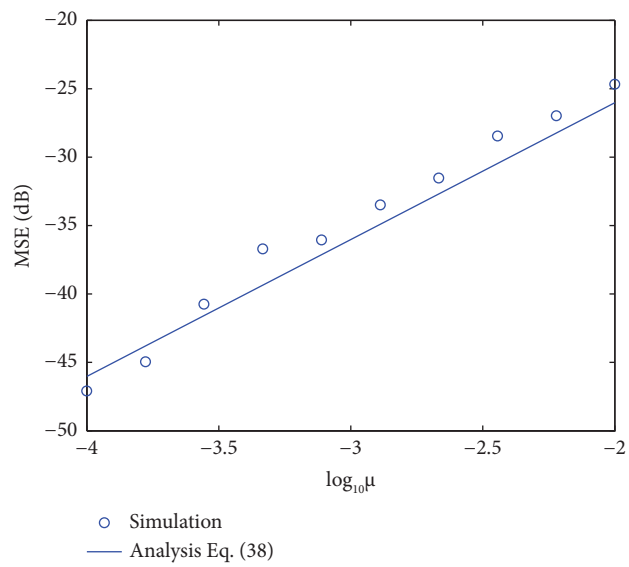

Figure 6: MSE as a function of step-size for $\mathrm{SNR}_i = 0\,\mathrm{dB}$, $\omega_0 = 0.5\pi$, $L = 10000$ and 100 runs.

power spectrum of a noise process with a few impulses per second. Impulsive noise is therefore a binary-state, time-varying process, and as a result, its power spectrum and autocorrelation are also binary-state processes. The expression for an amplitude-modulated binary-state sequence that models an impulsive noise sequence is [30].

$$I(n) = u(n)b(n), \tag{40}$$

where $u(n)$ is a random noise amplitude and $b(n)$ is a binary-state sequence of ones and zeros. Since the binary-state sequence $b(n)$ takes a value of "1" with a probability of p and a value of "0" with a probability of $1 - p$, its probability mass function (PMF) can be expressed as follows:

$$f(b) = \begin{cases} p, & b(n) = 1, \\ 1 - p, & b(n) = 0, \end{cases} \tag{41}$$

which is in the form of a Bernoulli distribution whose mean is p and variance is $p(1 - p)$ whereas the probability density function (PDF) of $u(n)$ can be modelled as a Gaussian distribution with a zero mean and variance of σ_u^2 and is of the form

$$f(u) = \frac{1}{\sigma_u \sqrt{2\pi}} e^{-u^2(n)/2\sigma_u^2}. \tag{42}$$

Since $u(n)$ and $b(n)$ are independent random variables, the variance of $I(n)$ can then be defined by (see Appendix D)

$$\sigma_I^2 = p\sigma_u^2. \tag{43}$$

It is noted that the mean of $I(n)$ is equal to zero because $u(n)$ has a zero mean. Therefore, equation (43) is also the impulsive noise power. Under the impulsive noise scenario, the observation signal in equation (1) can then be rewritten as follows:

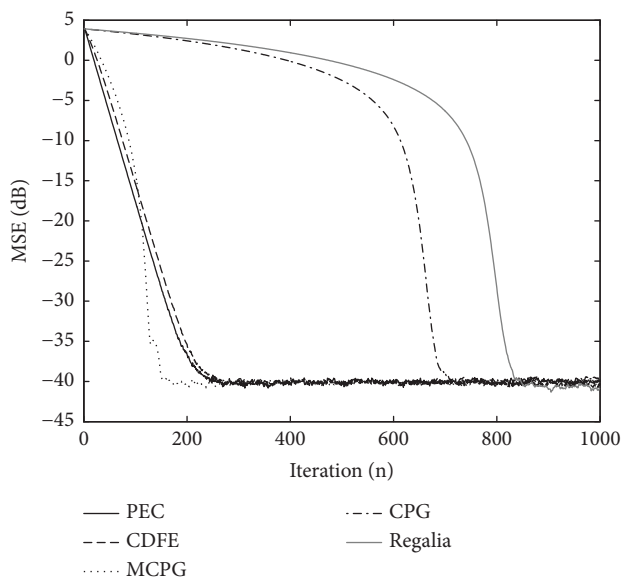

Figure 7: MSE of the estimated frequency for $\mathrm{SNR}_i = 10\,\mathrm{dB}$, $\omega_0 = 0.5\pi$, $\mu_{\mathrm{pec}} = 0.05$, $\mu_{\mathrm{cdfe}} = 0.025$, $\mu_{\mathrm{mcpg}} = 0.0175$, $\mu_{\mathrm{cpg}} = 0.02$, $\mu_{\mathrm{regalia}} = 0.004$, data length $L = 1000$ and 1000 runs.

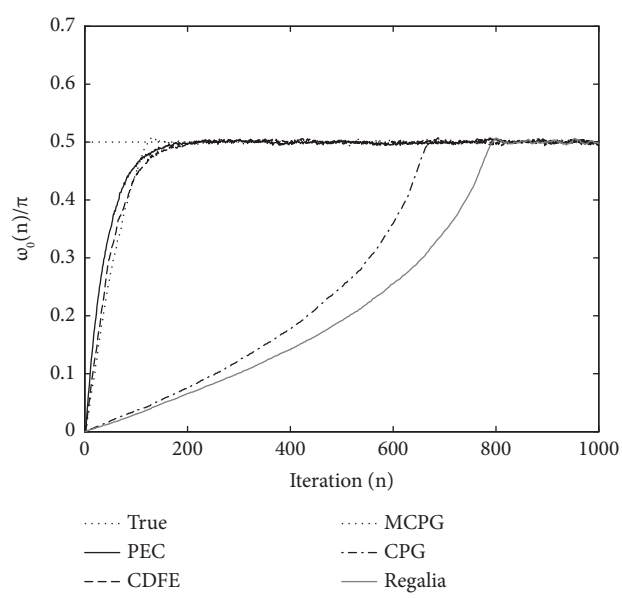

Figure 8: Learning curves of the estimated frequency for $\mathrm{SNR}_i = 10\,\mathrm{dB}$, $\omega_0 = 0.5\pi$, $\mu_{\mathrm{pec}} = 0.05$, $\mu_{\mathrm{cdfe}} = 0.025$, $\mu_{\mathrm{mcpg}} = 0.0175$, $\mu_{\mathrm{cpg}} = 0.02$, $\mu_{\mathrm{regalia}} = 0.004$ and data length $L = 1000$ and single run.

$$x(n) = d(n) + I(n). \tag{44}$$

The signal to impulsive noise ratio (SINR) is defined by

$$\begin{aligned}\mathrm{SINR} &= \frac{P_{\mathrm{signal}}}{P_{\mathrm{impulse}}} \\ &= \frac{A^2}{p\sigma_u^2}.\end{aligned} \tag{45}$$

From equation (45), there are many pairs of p and σ_u^2 that yield the same SINR. For a fixed value of σ_u^2, the lower the probability p is, the higher the SINR is achieved. Since the impulsive noise is nonstationary, it is difficult to theoretically study the proposed PEC algorithm under this noise. Therefore, experimentation by means of computer simulation is used to study the PEC performance under impulsive noise instead. Extensive simulations for low/high p and large σ_u^2 will be carried out to demonstrate the impulsive noise robustness of the proposed PEC adaptive algorithm. The

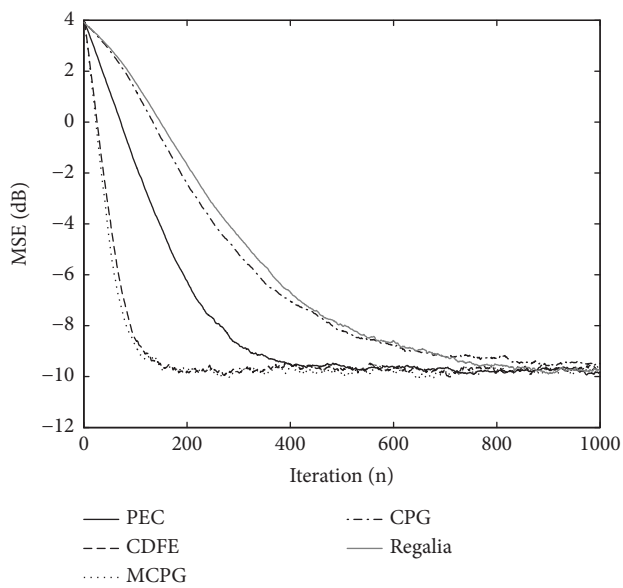

Figure 9: MSE of the estimated frequency for $\mathrm{SNR}_i = -5\,\mathrm{dB}$, $\omega_0 = 0.5\pi$, $\mu_{\mathrm{pec}} = 0.05$, $\mu_{\mathrm{cdfe}} = 0.032$, $\mu_{\mathrm{mcpg}} = 0.035$, $\mu_{\mathrm{cpg}} = 0.071$, $\mu_{\mathrm{regalia}} = 0.016$, data length $L = 1000$ and 5000 runs.

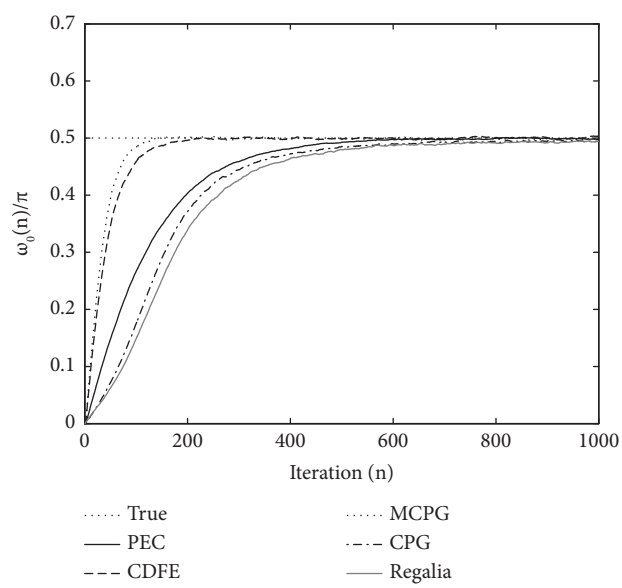

Figure 10: Learning curves of the estimated frequency $\mathrm{SNR}_i = -5\,\mathrm{dB}$, $\omega_0 = 0.5\pi$, $\mu_{\mathrm{pec}} = 0.05$, $\mu_{\mathrm{cdfe}} = 0.032$, $\mu_{\mathrm{mcpg}} = 0.035$, $\mu_{\mathrm{cpg}} = 0.071$, $\mu_{\mathrm{regalia}} = 0.016$, data length $L = 1000$ and 5000 runs.

Table 1: The computational complexity and computational time.

Algorithm	Computational complexity		Phase evaluation	Computational time
	Multiplication	Addition		
PEC	$3L$	$2L$	L	$O\,(6L)$
CDFE	$4L$	$2L$	—	$O\,(6L)$
MCPG	$6L$	$3L$	—	$O\,(9L)$
CPG	$7L$	$4L$	—	$O\,(11L)$
Regalia	$10L$	$3L$	—	$O\,(13L)$

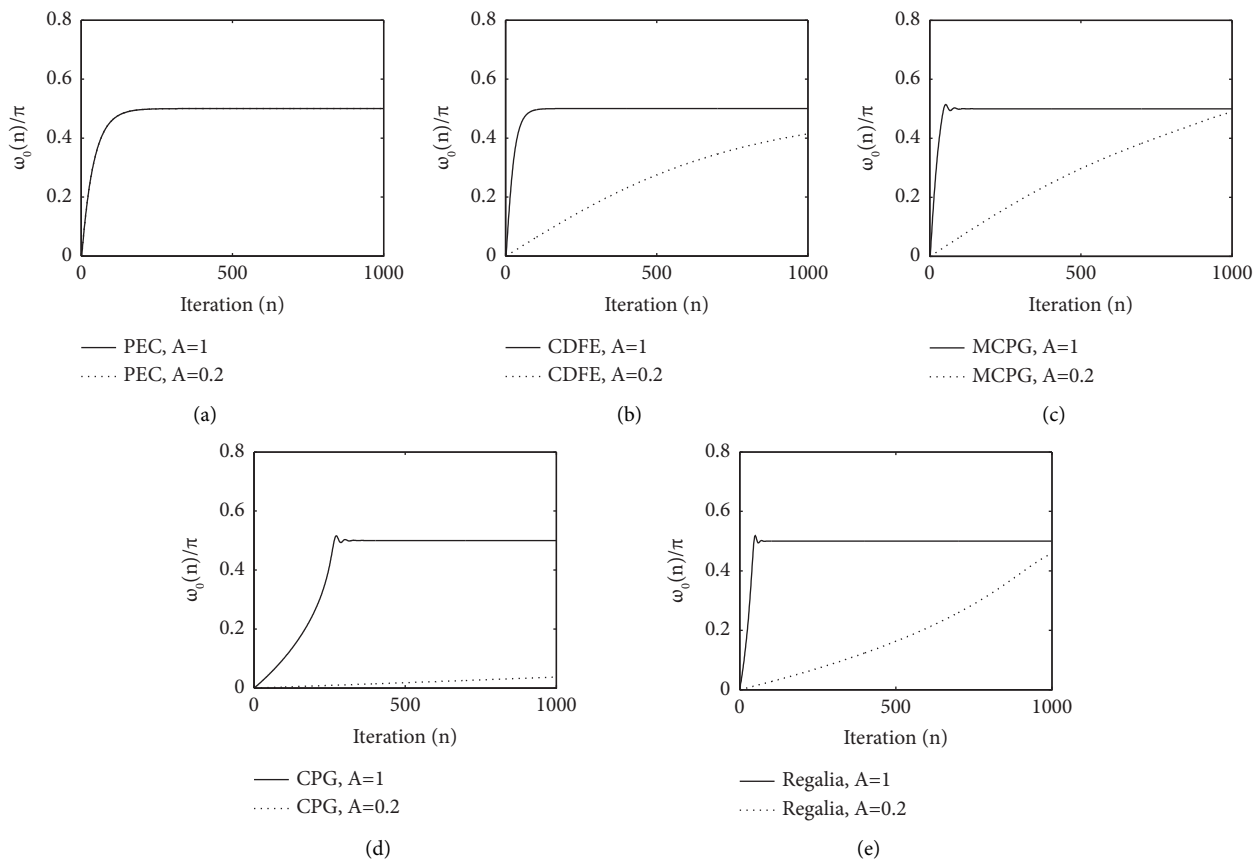

Figure 11: Deteriorating convergence speed due to the signal amplitude: (a) PEC; (b) CDFE; (c) MCPG; (d) CPG; and (e) Regalia.

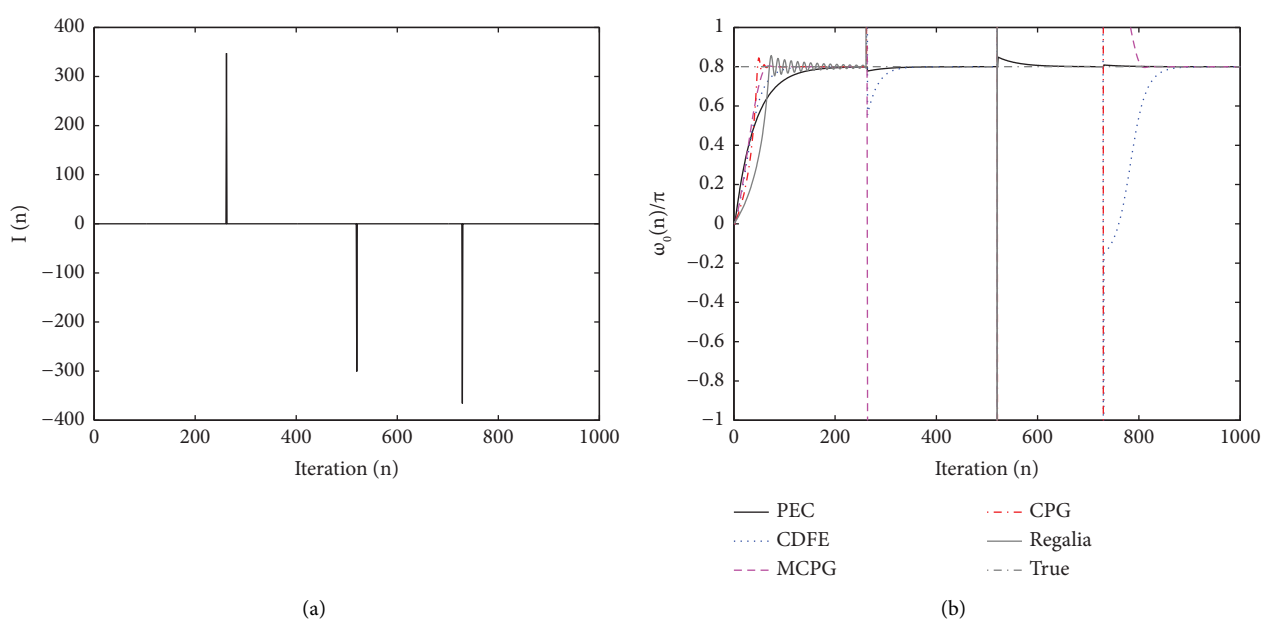

Figure 12: (a) Low probability large variance impulsive noise with SINR = −20 dB; (b) evolutions of the estimated frequency obtainable by the PEC, MCPG, CPG and Regalia for $\omega_0 = 0.8\pi$, $\mu_{\text{cdfe}} = 0.05$ and $\mu_{\text{mcpg}} = 0.05$ $\mu_{\text{cpg}} = 0.35$ and $\mu_{\text{regalia}} = 0.1$.

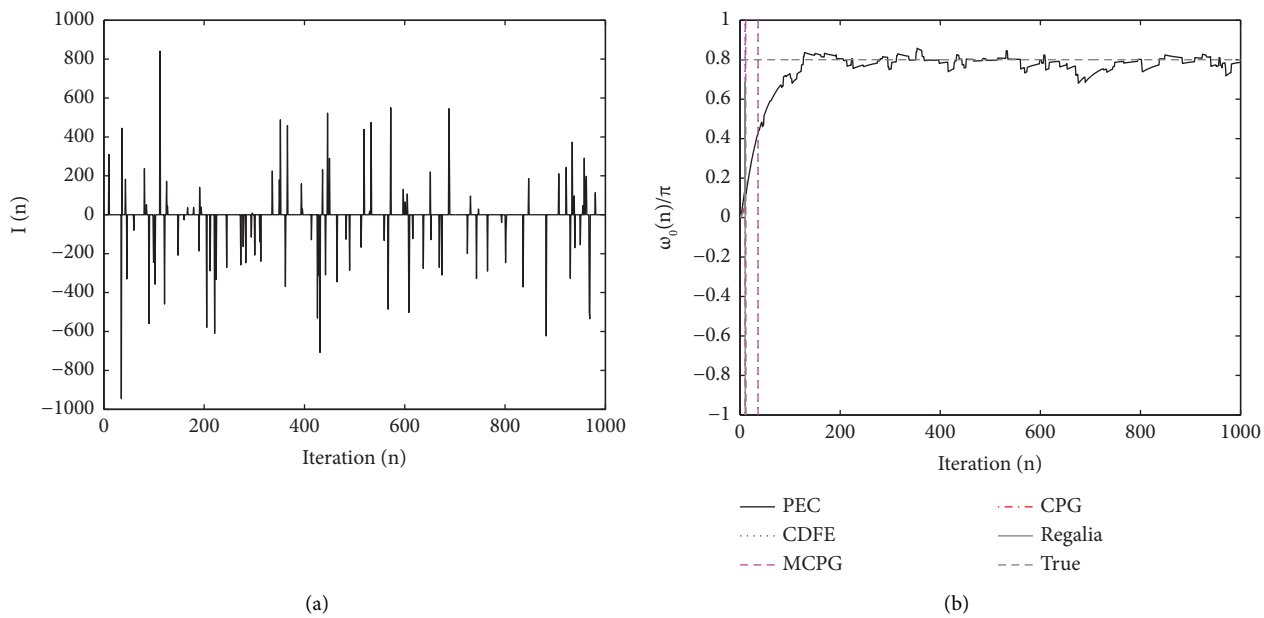

Figure 13: (a) High probability large variance impulsive noise of SINR = −40 dB; (b) evolutions of the estimated frequency obtainable by the PEC, MCPG, CPG, and Regalia for, $\omega_0 = 0.8\pi$, $\mu_{\text{cdfe}} = 0.05$, and $\mu_{\text{mcpg}} = 0.05$ $\mu_{\text{cpg}} = 0.35$ and $\mu_{\text{regalia}} = 0.1$.

simulations are addressed by considering the following cases: (note that the step-size parameter μ of each algorithm is individually adjusted to obtain the same convergence speed).

5.2.1. C1 Low Probability of Occurrence and Large Noise Amplitude Variance. For this case, we let $p = 0.001$ and $\sigma_u^2 = 10^5$ (SINR = −20 dB). The results of the estimation are shown in Figures 12(a) and 12(b). An impulsive noise waveform is shown in Figure 12(a). The estimated frequency obtained from the PEC, CDFE, MCPG, CPG, and Regalia are shown in Figure 12(b). It is evident that the proposed PEC is robust to very high impulsive noise, whereas the CDFE, MCPG, CPG, and Regalia suffer from impulsive noise; namely, they are not robust.

5.2.2. C2 High Probability and Large Noise Amplitude Variance. For this case we let $p = 0.1$ and $\sigma_u^2 = 10^5$ (SINR = −40 dB). The results of the estimation are shown in Figure 13(a) and 13(b). An impulsive noise waveform is shown in Figure 13(a). The estimated frequency obtained from the PEC, CDFE, MCPG, CPG, and Regalia are shown in Figure 13(b). It is evident that the proposed PEC is robust to very high impulsive noise, whereas the CDFE, MCPG, CPG, and Regalia suffer from impulsive noise; namely, they are unstable.

5.3. Effect of Signal Amplitude. To study the deterioration of convergence speed due to the signal amplitude A, a noise free scenario is assumed. The parameters used in simulation are $A = \{0.2, 1\}$, $\omega_0 = 0.5\pi$, $\varphi = 0.1\pi$, $\mu = 0.05$, $\alpha = 0.7$ (for MCPG, CPG, Regalia), and single run. The results are shown in Figure 11. As can be seen, the decrease in input signal amplitude does not affect the convergence speed of the proposed PEC (see Figure 11(a)), whereas the decrease in signal amplitude results in the deterioration of the convergence speed of the CDFE, MCPG, CPG, and Regalia (see Figures 11(b)–11(e)).

6. Conclusion

We have proposed a phase error criterion adaptive algorithm for estimating the unknown frequency of a complex sinusoidal signal. The proposed technique provides two main advantages: it is robust to impulsive noise and not very sensitive to the signal amplitude. The convergence in the mean of the estimated frequency and steady-state expression

for MSE are derived in closed form. Extensive studies using computer simulations have been conducted to show the superiority of the proposed adaptive algorithm.

Appendix

A. The derivation of equation (10)

Referring to equations (1) and (6)

$$\begin{aligned} x(n)x^*(n) - x(n)\hat{s}^*(n) &= (d(n)+v(n)) \times \left(d^*(n)+v^*(n)\right) \\ &\quad + (d(n)+v(n)) \times \left(e^{-j\hat{\omega}_0}\left(d^*(n-1)+v^*(n-1)\right)\right) \\ &= d(n)d^*(n) + v(n)v^*(n) + v(n)d^*(n) \\ &\quad + v^*(n)d(n) + e^{-j\hat{\omega}_0}d(n)d^*(n-1) \\ &\quad + e^{-j\hat{\omega}_0}d(n)v^*(n-1) + e^{-j\hat{\omega}_0}v(n)d^*(n-1) \\ &\quad + e^{-j\hat{\omega}_0}v(n)v^*(n-1). \end{aligned} \tag{A.1}$$

Averaging equation (A.1) yields

$$\begin{aligned} &E\left[d(n)d^*(n)\right] + E\left[v(n)v^*(n)\right] + e^{-j\hat{\omega}_0}E\left[d(n)d^*(n-1)\right] \\ &\quad = A^2 + \sigma^2 + A^2e^{-j\hat{\omega}_0}e^{j\omega_0} = A^2 + \sigma^2 + A^2e^{-j\left(\hat{\omega}_0-\omega_0\right)} \\ &\quad = A^2\left(1+\cos\delta_\omega\right) + \sigma^2 - jA^2\sin\delta_\omega. \end{aligned} \tag{A.2}$$

Evaluating equation (A.2) for the phase yields equation (10). Note that equation (A.2) is obtained by assuming that $d(n)$ and $v(n)$ are uncorrelated with each other and $e^{j\hat{\omega}_0}$ is a constant.

B. The derivation of equation (16)

The solution of equation (14) is given by

$$\bar{\omega}_0(n) = \bar{\omega}_{0c}(n) + \bar{\omega}_{0p}(n), \tag{A.3}$$

where $\bar{\omega}_{0c}(n)$ and $\bar{\omega}_{0p}(n)$ are, respectively, complementary and particular solutions. Assuming that the complementary solution takes the form of

$$\bar{\omega}_{0c}(n) = C\lambda^n, \quad n > 0, \tag{A.4}$$

where C is a constant determined by an initial condition. Letting the term on the right-hand side of equation (14) to be zeros and using equation (A.3) yields

$$\bar{\omega}_{0c}(n) = C\left(1-\mu\eta_0\right)^n, \quad n > 0. \tag{A.5}$$

In addition, it can be assumed that

$$\bar{\omega}_{0p}(n) = K\mu\eta_0\omega_0, \tag{A.6}$$

where K is a constant. After substituting equations (A.6) into (14) and solving the result, we obtain

$$\bar{\omega}_{0p}(n) = \omega_0. \tag{A.7}$$

Using equations (A.6) and (A.7) in equation (A.5) and solving for C results in equation (16) where $\bar{\omega}_0(0)$ is an initial condition.

C. The derivation of equation (29)

Referring to the power spectral theorem [11], the correlation between the noise components $v(n)$ and $v_1(n)$ can be computed by

$$\begin{aligned} R_{vv_1^*} &= \frac{\sigma^2}{2\pi}\int_{-\pi}^{\pi} H^*(\omega)d\omega, \\ &= \frac{\sigma^2}{2\pi}\left(2\pi - 2\sin(\pi)e^{-j\omega_0}\right) \\ &= \sigma^2 = \text{Eq. (29)}. \end{aligned} \tag{A.8}$$

D. The derivation of equation (43)

Since the impulsive noise $I(n)$ is the multiplication of two independent noise processes $u(n)$ and $b(n)$, the variance of $I(n)$ can be calculated by

$$\begin{aligned} \mathrm{Var}(I) &= \mathrm{Var}(ub) \\ &= \mathrm{Var}(u)\mathrm{Var}(b) + \mathrm{Var}(u)E^2[b] + \mathrm{Var}(b)E^2[u] \\ &= \sigma_u^2 p(1-p) + \sigma_u^2 p^2 \\ &= p\sigma_u^2 = \text{Eq. (43)}. \end{aligned} \tag{A.9}$$

Note that the time index n is omitted for analytical simplicity.

Data Availability

Due to laboratory policies, the data cannot be made public.

Conflicts of Interest

The authors declare that there are no conflicts of interest.

Authors' Contributions

Prayuth Inban and Rachu Punchalard conceptualized the study. Prayuth Inban proposed the methodology. Prayuth Inban is responsible for the software. Prayuth Inban, Rachu Punchalard, and Chawalit Benjangkaprasert validated the study. Prayuth Inban wrote the original draft. Prayuth Inban wrote, reviewed, and edited the study. Rachu Punchalard and Chawalit Benjangkaprasert visualized the study. Chawalit Benjangkaprasert supervised the study.

Acknowledgments

This study was supported by a student research grant (no contract) from school of engineering, King Mongkut's Institute of Technology Ladkrabang, Bangkok, Thailand.

References

[1] P. Stoica and R. Moses, *Introduction to Spectral Analysis*, Prentice-Hall, Upper Saddle River, NJ, USA, 1997.

[2] S. M. Kay, *Fundamentals of Statistical Signal Processing: Estimation Theory*, Prentice-Hall, Englewood Cliffs, NJ, USA, 1993.

[3] P. Pan, Y. Zhang, Z. Deng, and G. Wu, "Complex-Valued frequency estimation network and its applications to super-resolution of radar range profiles," *IEEE Transactions on Geoscience and Remote Sensing*, vol. 60, pp. 1–12, 2022.

[4] J. Kim, H. Ko, S. Hong, and C. Lee, "Fine Doppler frequency estimation of windowed complex sinusoidal signals for radar systems," *IEEE Sensors Journal*, vol. 21, no. 3, pp. 3860–3870, 2021.

[5] H. Song, Y. Bai, H. Wu, J. Liu, L. Fan, and J. Jin, "High-accuracy frequency estimation of sinusoid based on DFT and DTFT," in *Proceedings of the 2022 41st Chinese Control Conference (CCC)*, pp. 3107–3111, Hefei, China, July 2022.

[6] C. Wu, Y. Li, L. Luo, J. Xie, and L. Wang, "Two-step frequency estimation of GNSS signal in high dynamic environment," *International Journal of Antennas and Propagation*, vol. 2022, Article ID 1017206, 9 pages, 2022.

[7] B. Kim, S. Kim, and J. Lee, "A novel DFT-based DOA estimation by a virtual array extension using simple multiplications for FMCW radar," *Sensors*, vol. 18, no. 5, p. 1560, 2018.

[8] S. Lee and S. C. Kim, "Logarithmic-domain array interpolation for improved direction of arrival estimation in automotive radars," *Sensors*, vol. 19, no. 10, p. 2410, 2019.

[9] P. Stoica and A. Eriksson, "MUSIC estimation of real-valued sine-wave frequencies," *Signal Processing*, vol. 42, no. 2, pp. 139–146, 1995.

[10] L. B. Fertig and J. H. McClellan, "Instantaneous frequency estimation using linear prediction with comparisons to the DESAs," *IEEE Signal Processing Letters*, vol. 3, no. 2, pp. 54–56, 1996.

[11] V. F. Pisarenko, "The retrieval of harmonics from a covariance function," *Geophysical Journal International*, vol. 33, no. 3, pp. 347–366, 1973.

[12] H. C. So, "A close form frequency estimator for a noisy sinusoid," *Proceedings of 45th IEEE MWSC*, vol. 39, pp. 160–163, 2002.

[13] R. J. Kenefic and A. H. Nuttall, "Maximum likelihood estimation of the parameters of a tone using real discrete data," *IEEE Journal of Oceanic Engineering*, vol. 12, no. 1, pp. 279-280, 1987.

[14] Y. Liu, Z. Xu, H. Zhou, and Y. Zhao, "An efficient algorithm for frequency estimation of sinusoid signal based on improved quinn," *Journal of Physics: Conf. Ser*, vol. 1952, no. 4, Article ID 042094, 2021.

[15] R. Grover, A. Sharma, T. Delcourt, and D. Kundu, "Computationally efficient algorithm for frequency estimation of a two-dimensional sinusoidal model," *Circuits, Systems, and Signal Processing*, vol. 41, no. 1, pp. 346–371, 2022.

[16] H. C. So, "A comparative study of three recursive least-squares algorithms for single-tone frequency tracking," *Signal Processing*, vol. 83, no. 9, pp. 2059–2062, 2003.

[17] H. C. So and P. C. Ching, "Adaptive algorithm for direct frequency estimation," *IEE Proceedings Radar, Sonar and Navigation*, vol. 151, no. 6, pp. 359–364, 2004.

[18] R. Prony, "Experimentale et analytique," pp. 24–76, 1795, https://users.polytech.unice.fr/%7Eleroux/PRONY.pdf.

[19] G. W. Lank, I. S. Reed, and G. E. Pollon, "A semicoherent detection and Doppler estimation statistic," *IEEE Transactions on Aerospace and Electronic Systems*, vol. 9, no. 2, pp. 151–165, 1973.

[20] S. Kay, "A fast and accurate single frequency estimator," *IEEE Transactions on Acoustics, Speech, and Signal Processing*, vol. 37, no. 12, pp. 1987–1990, 1989.

[21] H. C. So and F. K. W. Chan, "A generalized weighted linear predictor frequency estimation approach for a complex sinusoid," *IEEE Transactions on Signal Processing*, vol. 54, no. 4, pp. 1304–1315, 2006.

[22] H. C. So, K. W. Chan, and W. Sun, "Subspace approach for fast and accurate single-tone frequency estimation," *IEEE Transactions on Signal Processing*, vol. 59, no. 2, pp. 827–831, 2011.

[23] A. Nosan and R. Punchalard, "A complex adaptive notch filter using modified gradient algorithm," *Signal Processing*, vol. 92, no. 6, pp. 1508–1514, 2012.

[24] P. A. Regalia, "A complex adaptive notch filter," *IEEE Signal Processing Letters*, vol. 17, no. 11, pp. 937–940, 2010.

[25] S. Nishimura and H.-Y. Jiang, "Gradient-based complex adaptive IIR notch filters for frequency estimation," in *Proceedings of the IEEE APCCAS*, Seoul, Korea, November 1996.

[26] A. Mvuma, T. Hinamoto, and S. Nishimura, "Gradient-based algorithm for a complex coefficient adaptive IIR notch filter: steady-state analysis and application," in *Proceedings of the 47th IEEE MWSC*, Hiroshima, Japan, July 2004.

[27] R. Punchalard and P. Wardkein, "Linear prediction based adaptive algorithm for a complex sinusoidal frequency

estimation," *AEU International Journal of Electronics and Communications*, vol. 67, no. 6, pp. 521–527, 2013.

[28] A. V. Oppenheim and R. W. Scharfer, *Digital Signal Processing*, Prentice-Hall, London, UK, 1975.

[29] M. P. Fitz, "Further results in the fast estimation of a single frequency," *IEEE Transactions on Communications*, vol. 42, no. 2/3/4, pp. 862–864, 1994.

[30] V. Saeed, *Vaseghi, Advanced Digital Signal Processing and Noise Reduction*, John Wiley and Sons Ltd, Hoboken, NJ, USA, 2000.